

Catalytic Oligomerization of Ethylene to Higher Linear α -Olefins Promoted by Cationic Group 4 Cyclopentadienyl-Arene Active Catalysts: Toward the Computational Design of Zirconium- and Hafnium-Based Ethylene Trimerization Catalysts

Sven Tobisch*,† and Tom Ziegler‡

Institut für Anorganische Chemie der Martin-Luther-Universität Halle-Wittenberg, Fachbereich Chemie, Kurt-Mothes-Strasse 2, D-06120 Halle, Germany, and Department of Chemistry, University of Calgary, University Drive 2500, Calgary, Alberta, Canada T2N 1N4

Received August 17, 2004

A detailed computational exploration is presented of the catalytic abilities of heavier group 4 ($M = \text{Zr}, \text{Hf}$) mono(boratabenzene-arene) compounds for linear ethylene oligomerization with the cationic $[(\eta^6\text{-BC}_5\text{H}_5)\text{-(bridge)-C}_6\text{H}_5]\text{M}^{\text{II}}(\text{C}_2\text{H}_4)_2]^+$ complex as active catalyst species, employing a gradient-corrected DFT method. The influence of the boron substitution on the cyclopentadienyl moiety and the length of the boratabenzene-arene connecting bridge on the energy profile of the oxidative coupling and the competing metallacycle growth and decomposition steps has been elucidated. This allowed us to suggest promising modifications of the parent Cp-based Ti analogue, which has been described by Hessen and co-workers as a catalyst for ethylene trimerization, thereby contributing to the computer-based rational design of improved group 4 oligomerization catalysts. The boratabenzene Zr compound bearing a CMe_2 -bridge is indicated to be an efficient trimerization catalyst, which should exhibit an activity that exceeds what is reported for the established Ti system. The computational probing reveals for the Hf counterpart a catalytic ability that is different. This system is suggested to possess catalytic potential for production of 1-octene besides the prevalent 1-hexene oligomer product. Electronic modification of the substituent on boron can act to modulate the α -olefin product composition toward an enhanced 1-octene portion, although not as the predominant product.

Introduction

Higher ($\text{C}_4\text{--C}_{20}$) linear α -olefins are valuable and versatile feedstocks and building blocks for the chemical industry, produced in a megaton scale per year, that have a large and diverse field of applications.¹ They are of wide interest, among other applications, as monomers (C_{10} for production of poly- α -olefins) and as comonomers ($\text{C}_4\text{--C}_8$ to generate linear low-density LLDPE² polyeth-

ylene and as additives for high-density HDPE polyethylene production) in catalytic olefin polymerization,^{1,3} as well as in the manufacturing of surfactants ($\text{C}_{10}\text{--C}_{18}$).^{1c,e} Nowadays, oligomerization of the less expensive ethylene is the predominant route to α -olefins,^{1c,e,4} with the Shell higher olefin process (SHOP)⁵ as the principal industrial process.

Among the variety of known catalysts for ethylene oligomerization,^{6,7} most of them afford a broad Schulz–Flory distribution⁸ of α -olefins having different chain lengths. The development of efficient catalyst systems for the selective production of specific desirable α -olefins

* To whom correspondence should be addressed. E-mail: tobisch@chemie.uni-halle.de.

† Martin-Luther-Universität Halle-Wittenberg.

‡ University of Calgary.

(1) (a) Weissert, K.; Arpe, H.-J. In *Industrial Organic Chemistry. Important Raw Materials and Intermediates*; Verlag Chemie: Weinheim, 1978. (b) Parshall, G. W.; Ittel, S. D. In *Homogeneous Catalysis, The Applications and Chemistry of Catalysis by Soluble Transition Metal Complexes*; John Wiley & Sons: New York, 1992; p 56. (c) Al-Jarallah, A. H.; Anabtawi, J. A.; Siddiqui, M. A. B.; Aitani, A. M.; Al-Sadoun, A. W. *Catal. Today* **1992**, *14*, 1. (d) Bhaduri, S.; Mukesh, D. In *Homogeneous Catalysis, Mechanisms and Industrial Applications*; John Wiley & Sons: New York, 2000; pp 142–147. (e) Vogt, D. Oligomerization of Ethylene to Higher Linear α -Olefins. In *Applied Homogeneous Catalysis with Organometallic Complexes*; Cornils, B., Herrmann, W. A., Eds.; VCH: Weinheim, Germany, 2002; pp 240–253.

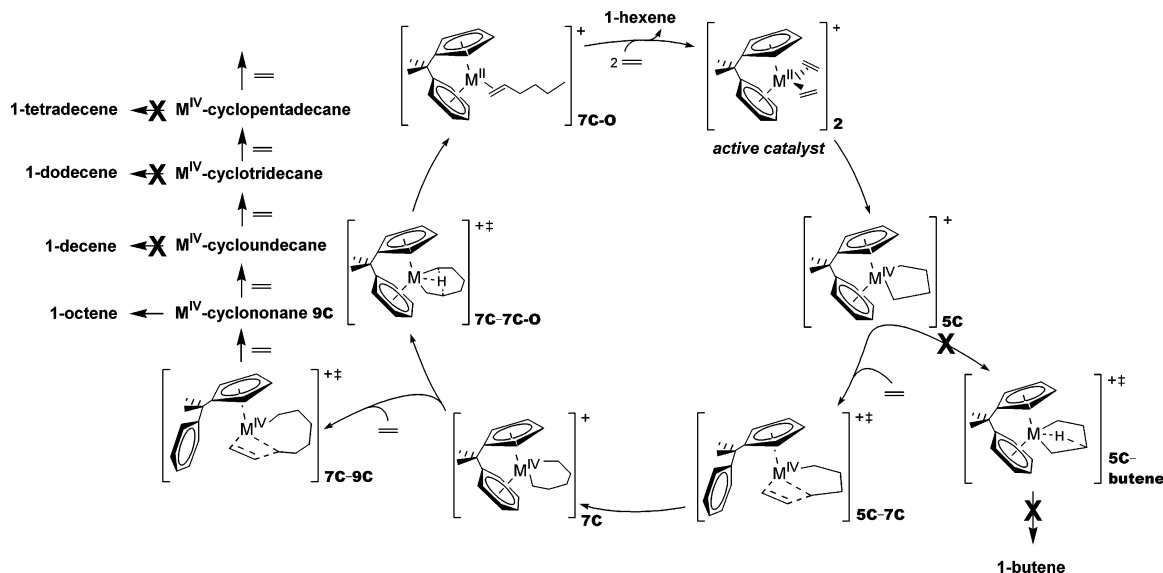
(2) (a) Tait, P. J. T.; Berry, I. G. In *Comprehensive Polymer Science*; Eastmond, G. C., Ledwith, A., Russo, S., Sigwalt, P., Eds.; Pergamon: Oxford, U.K., 1989; Vol. 4, p 575. (b) *Encyclopedia of Polymer Science and Engineering*; Mark, H. F., Bikales, N. B., Overberger, C. G., Menges, G., Kroschwitz, J. I., Eds.; John Wiley & Sons: New York, 1986; Vol. 6, p 429.

(3) Hennico, A.; Leonard, J.; Forestire, A.; Glaize, Y. *Hydrocarbon Process* **1990**, *69*, 73.

(4) (a) Onsager, O.-T.; Johansen, J. E. In *The Chemistry of the Metal–Carbon Bond*; Hartley, F. R., Patai, F. R., Eds.; John Wiley & Sons: Chichester, U.K., 1986; Vol. 3 p 205. (b) Skupinska, J. *Chem. Rev.* **1991**, *91*, 613. (c) Olivier-Bourbigou, H.; Saussine, L. Dimerization and Codimerization. In *Applied Homogeneous Catalysis with Organometallic Complexes*; Cornils, B., Herrmann, W. A., Eds.; VCH: Weinheim, Germany, 2002; pp 253–265.

(5) (a) Keim, W.; Kowaldt, F. H. *Erdöl Erdgas Kohle* **1978**, *78–79*, 453. (b) Keim, W.; Kowaldt, F. H.; Goddard, R.; Krüger, C. *Angew. Chem., Int. Ed. Engl.* **1978**, *17*, 466. (c) Freitas, E. R.; Gum, C. R. *Chem. Eng. Prog.* **1979**, *75*, 73. (d) Keim, W. *Chem. Ing. Technol.* **1984**, *56*, 850. (e) Keim, W. *New J. Chem.* **1987**, *11*, 531. (f) Keim, W. *Angew. Chem., Int. Ed. Engl.* **1990**, *29*, 235. (g) Keim, W. *Makromol. Chem. Macromol. Symp.* **1993**, *66*, 225. (h) Vogt, D. SHOP Process In *Aqueous-Phase Organometallic Catalysts, Concepts and Applications*; Cornils, B., Herrmann, W. A., Eds.; VCH: Weinheim, Germany, 1998; pp 541–547.

Scheme 1. Theoretically Refined Catalytic Cycle for the Linear Oligomerization of Ethylene Mediated by the Cationic Heavier Group 4 $[(\eta^5\text{-Cp}(\text{-bridge-Ph})\text{M}^{\text{II}}(\text{ethylene})_2]^+$ Active Catalysts (M = Zr, Hf)^{a,14b}



^a Based on a proposal by Hessen et al. for the Ti-catalyzed process.^{12a,b}

has recently triggered intensive research in both academia and industry. However, there have been only a limited number of reports of the selective ethylene trimerization to 1-hexene with catalysts that are based on chromium,⁹ tantalum,¹⁰ and titanium.^{11–13}

Hessen and co-workers described monocyclopentadienyl titanium complexes bearing a hemilabile ancillary arene functionality as precatalysts for ethylene trimerization.^{12a–c} The cationic $[(\eta^5\text{-Cp}(\text{-CMe}_2\text{-bridge})\text{-C}_6\text{H}_5)\text{-Ti}^{\text{IV}}(\text{alkyl})_2]^+$ species with a dimethyl-substituted C₁-bridge connecting the Cp ring with the pendant phenyl

group has been observed as a particularly active and selective trimerization precatalyst.^{12b} This class of catalysts has recently been the subject of computational investigations by us¹⁴ and other groups.¹⁵ These studies verified for the most part the catalytic cycle proposed by Hessen and co-workers.^{12a,b} The mechanism involves metallacycle intermediates, similar to that originally suggested by Briggs and Jolly for Cr-based catalysts.^{16,17} Furthermore, the crucial role played by the hemilabile phenyl group in order to make the metallacycle mechanism operative has been clarified, and a detailed insight into the discriminating factors that control the highly selective 1-hexene formation has been provided.^{14a} In a subsequent investigation we have probed computationally the catalytic abilities of the related Zr- and Hf-based catalysts for linear ethylene oligomerization,^{14b} although their potential has not yet been explored experimentally. This study suggested the CMe₂-bridged Zr system, unlike the parent Ti catalyst, as a promising catalyst possessing potential for production of 1-octene besides the prevalent 1-hexene oligomer product. Scheme 1 shows the theoretically refined catalytic cycle for the ethylene oligomerization mediated by these heavier group 4 catalysts.^{14b} Further explorations covered the theoretical analysis of the influence of substitutions of the hemilabile arene functionality on the energy profiles

(6) For past reviews see: (a) Keim, W.; Behr, A.; Röper, M. Alkene and Alkyne Oligomerization, Cooligomerization and Telomerization Reactions. In *Comprehensive Organometallic Chemistry*; Wilkinson, G., Stone, F. G. A., Abel, E. W., Eds.; Pergamon: New York, 1982; Vol. 8, pp 371–462. (b) Jolly, P. W. Nickel-Catalyzed Oligomerization of Alkenes and Related Reactions. In *Comprehensive Organometallic Chemistry*; Wilkinson, G., Stone, F. G. A., Abel, E. W., Eds.; Pergamon: New York, 1982; Vol. 8, pp 615–647.

(7) For recent reviews see: (a) Britovsek, G. J. P.; Gibson, V. C.; Wass, D. F. *Angew. Chem., Int. Ed.* **1999**, *38*, 428. (b) Ittel, S. D.; Johnson, L. K.; Brookhart, M. *Chem. Rev.* **2000**, *100*, 1169. (c) Mecking, S. *Coord. Chem. Rev.* **2000**, *203*, 325. (d) Mecking, S. *Angew. Chem., Int. Ed.* **2001**, *40*, 534. (e) Gibson, V. C.; Spitzmesser, S. K. *Chem. Rev.* **2003**, *103*, 283.

(8) (a) Flory, P. J. *J. Am. Chem. Soc.* **1940**, *62*, 1561. (b) Schulz, G. V. *Z. Phys. Chem., Abt. B* **1935**, *30*, 379. (c) Schulz, G. V. *Z. Phys. Chem., Abt. B* **1939**, *43*, 25.

(9) (a) Hogan, J. P. *J. Polym. Sci. A* **1970**, *8*, 2637. (b) Manyik, R. M.; Walker, W. E.; Wilson, T. P. *J. Catal.* **1977**, *47*, 197. (c) Yang, Y.; Kim, H.; Lee, J.; Paik, H.; Jang, H. G. *Appl. Catal. A Gen.* **2000**, *193*, 29. (d) Köhn, R. D.; Haufe, M.; Kociok-Köhn, G.; Grimm, S.; Wasserscheid, P.; Keim, W. *Angew. Chem., Int. Ed.* **2000**, *39*, 4337. (e) Monoi, T.; Sasaki, Y. *J. Mol. Catal. A: Chem.* **2002**, *187*, 135. (f) Carter, A.; Cohen, S. A.; Cooley, N. A.; Murphy, A.; Scutt, J.; Wass, D. F. *J. Chem. Soc., Chem. Commun.* **2002**, 858. (g) McGuinness, D. S.; Wasserscheid, P.; Keim, W.; Morgan, D.; Dixon, J. T.; Bollmann, A.; Maumela, H.; Hess, F.; Englert, U. *J. Am. Chem. Soc.* **2003**, *125*, 5272. (h) McGuinness, D. S.; Wasserscheid, P.; Keim, W.; Hu, Ch.; Englert, U.; Dixon, J. T.; Grove, C. *J. Chem. Soc., Chem. Commun.* **2003**, 334. (i) Morgan, D. H.; Schwikkard, S. L.; Dixon, J. T.; Nair, J. J.; Hunter, R. *Adv. Synth. Catal.* **2003**, *345*, 939. (j) Mahomed, H.; Bollmann, A.; Dixon, J. T.; Gokul, V.; Griesel, L.; Grove, C.; Hess, F.; Maumela, H.; Pepler, L. *Appl. Catal. A: Gen.* **2003**, *255*, 355. (k) Morgan, D. H.; Schwikkard, S. L.; Dixon, J. T.; Nair, J. J.; Hunter, R. *Adv. Synth. Catal.* **2003**, *345*, 939. (l) Agapi, T.; Schofer, S. J.; Labinger, J. A.; Bercaw, J. E. *J. Am. Chem. Soc.* **2004**, *126*, 1304.

(10) Andes, C.; Harkins, S. B.; Murtuza, K. O.; Sen, A. *J. Am. Chem. Soc.* **2001**, *123*, 7423.

(11) Pellecchia, C.; Pappalardo, D.; Oliva, L.; Mazzeo, M.; Gruter, G.-J. *Macromolecules* **2000**, *33*, 2807.

(12) (a) Deckers, P. J. W.; Hessen, B.; Teuben, J. H. *Angew. Chem., Int. Ed.* **2001**, *40*, 2516. (b) Deckers, P. J. W.; Hessen, B.; Teuben, J. H. *Organometallics* **2002**, *21*, 5122. (c) Hessen, B. *J. Mol. Catal. A: Chem.* **2004**, *213*, 129. (d) The actual reaction conditions for the Ti-catalyzed selective trimerization of ethylene to 1-hexene are: 30 °C, ethylene pressure 5 bar, toluene as solvent.

(13) (a) Huang, J.; Wu, T.; Qian, Y. *J. Chem. Soc., Chem. Commun.* **2003**, 2816. (b) Wu, T.; Qian, Y.; Huang, J. *J. Mol. Catal. A: Chem.* **2004**, *214*, 227.

(14) (a) Tobisch, S.; Ziegler, T. *Organometallics* **2003**, *22*, 5392. (b) Tobisch, S.; Ziegler, T. *J. Am. Chem. Soc.* **2004**, *126*, 9059. (c) Tobisch, S.; Ziegler, T. *Organometallics* **2004**, *23*, 4077.

(15) (a) Blok, A. N. J.; Budzelaar, P. H. M.; Gal, A. W. *Organometallics* **2003**, *22*, 2564. (b) de Bruin, T. J. M.; Magna, L.; Raybaud, P.; Toulhoat, H. *Organometallics* **2003**, *22*, 3404.

(16) Briggs, J. R. *J. Chem. Soc., Chem. Commun.* **1989**, 674.

(17) (a) Jolly, P. W. *Acc. Chem. Res.* **1996**, *29*, 544. (b) Emrich, R.; Heinemann, O.; Jolly, P. W.; Krüger, C.; Verhovnik, G. P. *J. Organometallics* **1997**, *16*, 1511.

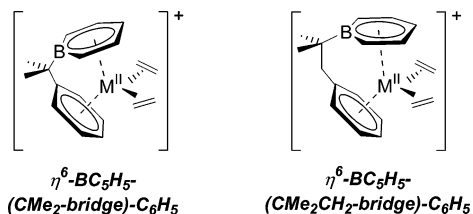


Figure 1. Explored cationic group 4 mono(boratabenzene-arene) [$(\eta^6\text{-BC}_5\text{H}_5\text{-}(\text{R-bridge})\text{-C}_6\text{H}_5)\text{M}^{\text{II}}\text{-(ethylene)}_2$] $^+$ ($\text{M} = \text{Zr, Hf}$; $\text{R} = \text{CMe}_2, \text{CMe}_2\text{CH}_2$) active catalyst complexes.

of crucial elementary steps for the Zr and Hf catalysts, thereby providing a detailed insight into how electronic modifications of the phenyl group act to modulate the product distribution.^{14c}

The present investigation continues our systematic theoretical exploration of the catalytic abilities of the heavier group 4 mono(cyclopentadienyl-arene) Zr and Hf compounds as catalysts for the linear ethylene oligomerization. Herein, we report the detailed evaluation of how the variation of the electronic nature of the Cp moiety controls the composition of the oligomer products. Unlike the common approach of introducing electron-releasing or -withdrawing substituents on the Cp ligand, we decided to study systems with a heteroatom-substituted Cp analogue. Among the variety of such ligands,¹⁸ the boratabenzene [HBC_5H_5] $^-$ and phospholyl [PC_4H_4] $^-$ anions are most common. Especially the former has been involved in a wide field of applications (vide infra). This prompted us to investigate the boratabenzene Zr and Hf compounds bearing a pendant phenyl group with a CMe_2 (C_1) and CMe_2CH_2 (C_2) bridge, shown in Figure 1, which represent the counterparts of the recently studied Cp-arene analogues.^{14b,c}

Boratabenzenes are six π -electron aromatic anions, which can serve as versatile ligands¹⁹ toward a variety of metals.^{20,21} Although the boratabenzene anion and the parent cyclopentadienyl anion are isoelectronic, they exhibit distinctly different electronic characteristics.²² The comparison of the frontier orbitals²³ reveals the boratabenzene anion to be the poorer π -donor,²⁰ which causes the metal center to be more electrophilic than in the parent M-Cp systems. On the other hand, boratabenzenes are characterized by a low-lying σ -ac-

ceptor orbital.^{23,24} Among the several catalytic applications, boratabenzene analogues of group 4 metallocenes,²⁵ *ansa*-metallocenes,²⁶ and “constrained geometry”²⁷ complexes are well-known, like the parent group 4 systems, to be active catalysts for olefin oligomerization and polymerization. Furthermore, boratabenzene compounds with group 3 and 6 metals as the active center have also been shown to promote these processes.²⁸ Noticeably, as demonstrated for group 4 bis-(boratabenzene) complexes, the substituent on boron seems to be an efficient handle by which to tune the rate of β -H elimination, thereby controlling whether oligomers or polymers are the predominant products.²⁵

The computational exploration of the catalytic abilities of heteroatom-substituted Cp-analogue systems presented here will enhance the understanding of the catalytic structure–reactivity relationships for ethylene oligomerization supported by the title class of group 4 catalysts. It is our goal to contribute to the rational computer-based design of Zr- and Hf-based catalysts for ethylene trimerization that might display catalytic activities beyond what is already reached for the reported Ti system.^{12a,b}

Computational Details

Method. All calculations have been performed with the program package TURBOMOLE²⁹ using density functional theory (DFT). The local exchange–correlation potential by Slater^{30a,b} and Vosko et al.^{30c} was augmented with gradient-corrected functionals for electron exchange according to Becke^{30d} and correlation according to Perdew^{30e} in a self-consistent fashion. This gradient-corrected density functional is usually termed BP86 in the literature. In recent benchmark computational studies it was shown that the BP86 functional gives results in excellent agreement with the best wave function-based methods available today, for the class of reactions investigated here.³¹ The appropriateness of the DFT(BP86) method for the reliable description of the kinetic balance between the metallacycle growth and decomposition steps of the group 4 metal-assisted ethylene oligomerization has been previously demonstrated,^{14b} thus validating the applied meth-

(18) See for instance: Ashe, A. J., III; Bajko, Z.; Carr, M. D.; Kampf, J. W. *Organometallics* **2003**, *22*, 910.

(19) (a) Herberich, G. E.; Greiss, G.; Heil, H. F. *Angew. Chem., Int. Ed. Engl.* **1970**, *9*, 805. (b) Ashe, A. J., III; Shu, P. *J. Am. Chem. Soc.* **1971**, *93*, 1804.

(20) (a) For early reviews, see: Herberich, G. E.; Ohst, H. *Adv. Organomet. Chem.* **1986**, *25*, 199. (b) Herberich, G. E. *Comprehensive Organometallic Chemistry II*; Abel, E. W., Stone, F. G. A., Wilkinson, G., Eds.; Pergamon Press: Oxford, U.K., 1995; Vol. 1, p 381. (c) For a recent review, see: Fu, G. C. *Adv. Organomet. Chem.* **2001**, *47*, 101.

(21) (a) Herberich, G. E.; Klein, W.; Spaniol, T. P. *Organometallics* **1993**, *12*, 2660. (b) Herberich, G. E.; Schmidt, B.; Englert, U. *Organometallics* **1995**, *14*, 471. (c) Hoic, D. A.; Davis, W. M.; Fu, G. C. *J. Am. Chem. Soc.* **1995**, *117*, 8480. (d) Herberich, G. E.; Englert, U.; Ganter, B.; Lamertz, C. *Organometallics* **1996**, *15*, 5236. (e) Herberich, G. E.; Englert, U.; Schmitz, A. *Organometallics* **1997**, *16*, 3751. (f) Sperry, C. K.; Rodriguez, G.; Bazan, G. C. *J. Organomet. Chem.* **1997**, *548*, 1. (g) Putzer, M. A.; Lachicotte, R. J.; Bazan, G. C. *Inorg. Chem. Commun.* **1999**, *2*, 319. (h) Herberich, G. E.; Englert, U.; Fischer, A.; Ni, J.; Schmitz, A. *Organometallics* **1999**, *18*, 5496.

(22) Ashe, A. J., III; Al-Ahmad, S.; Fang, X. G. *J. Organomet. Chem.* **1999**, *581*, 92.

(23) With the computational methodology applied here (DFT(BP86) + valence triple- ζ basis sets) the frontier orbitals of free Cp^- are at 0.97 eV (π HOMO) and 5.64 eV (π LUMO), while for the free boratabenzene anion they are at 0.18 eV (π HOMO) and 4.13 eV (σ LUMO), respectively.

(24) (a) Schulman, J. M.; Disch, R. L.; Sabio, M. L. *J. Am. Chem. Soc.* **1982**, *104*, 3785. (b) Raabe, G.; Schleker, W.; Heyne, E.; Fleischhauer, J. Z. *Naturforsch., A* **1984**, *39*, 678. (c) Raabe, G.; Schleker, W.; Heyne, E.; Fleischhauer, J. Z. *Naturforsch., A* **1987**, *42*, 352. (d) Schulman, J. M.; Disch, R. L. *Organometallics* **1989**, *8*, 733. (e) Cioslowski, J.; Hay, P. J. *J. Am. Chem. Soc.* **1990**, *112*, 1707. (f) Karadakov, P. B.; Ellis, M.; Gerratt, J.; Cooper, D. L.; Raimondi, M. *Int. J. Quantum Chem.* **1997**, *63*, 441.

(25) (a) Bazan, G. C.; Rodriguez, G.; Ashe, A. J., III; Al-Ahmad, S.; Müller, C. *J. Am. Chem. Soc.* **1996**, *118*, 2291. (b) Rogers, J. S.; Bazan, G. C.; Sperry, C. K. *J. Am. Chem. Soc.* **1997**, *119*, 9305. (c) Bazan, G. C.; Rodriguez, G.; Ashe, A. J., III; Al-Ahmad, S.; Kampf, J. W. *Organometallics* **1997**, *16*, 2492. (d) Lee, R. A.; Lachicotte, R. J.; Bazan, G. C. *J. Am. Chem. Soc.* **1998**, *120*, 6037.

(26) Ashe, A. J., III; Al-Ahmad, S.; Fang, X.; Kampf, J. W. *Organometallics* **1998**, *17*, 3883.

(27) Ashe, A. J., III; Fang, X.; Kampf, J. W. *Organometallics* **1999**, *18*, 1363.

(28) (a) Putzer, M. A.; Rogers, J. S.; Bazan, G. C. *J. Am. Chem. Soc.* **1999**, *121*, 8112. (b) Rogers, J. S.; Bu, X.; Bazan, G. C. *J. Am. Chem. Soc.* **2000**, *122*, 730. (c) Rogers, J. S.; Bu, X.; Bazan, G. C. *Organometallics* **2000**, *19*, 3948.

(29) (a) Ahlrichs, R.; Bär, M.; Häser, M.; Horn, H.; Kölmel, C. *Chem. Phys. Lett.* **1989**, *162*, 165. (b) Treutler, O.; Ahlrichs, R. *J. Chem. Phys.* **1995**, *102*, 346. (c) Eichkorn, K.; Treutler, O.; Öhm, H.; Häser, M.; Ahlrichs, R. *Chem. Phys. Lett.* **1995**, *242*, 652.

(30) (a) Dirac, P. A. M. *Proc. Cambridge Philos. Soc.* **1930**, *26*, 376. (b) Slater, J. C. *Phys. Rev.* **1951**, *81*, 385. (c) Vosko, S. H.; Wilk, L.; Nussiar, M. *Can. J. Phys.* **1980**, *58*, 1200. (d) Becke, A. D. *Phys. Rev.* **1988**, *A38*, 3098. (e) Perdew, J. P. *Phys. Rev.* **1986**, *B33*, 8822; *Phys. Rev. B* **1986**, *34*, 7406.

(31) Jensen, V. R.; Børve, K. *J. Comput. Chem.* **1998**, *19*, 947.

Table 1. Calculated Gibbs Free-Energy Profile (ΔG , ΔG^\ddagger in kcal mol⁻¹) for Formation and Growth of Group 4 Metallacycle Intermediates during the Linear Oligomerization of Ethylene Mediated by the Cationic [η^6 -BC₅H₅-(R-bridge)-C₆H₅]⁺M^{II}(C₂H₄)₂⁺ (M = Zr, Hf) Active Catalyst Complex^a

cycle growth	R-bridge	$\Delta G_{\text{XC-E}},^b$ M = Zr/Hf	$\Delta G^\ddagger,$ M = Zr/Hf	$\Delta G,$ M = Zr/Hf
M ^{II} -(C ₂ H ₄) ₂ → M ^{IV} -C ₄ H ₈	CMe ₂ -bridge		10.7/9.2	-5.7/-5.5
2 → 5C	CMe ₂ CH ₂ -bridge		10.7/9.4	-8.0/-7.7
M ^{IV} -C ₄ H ₈ → M ^{IV} -C ₆ H ₁₂	CMe ₂ -bridge	9.0/9.4	14.5/15.8	-9.8/-7.2
5C + C ₂ H ₄ → 5C-E → 7C	CMe ₂ CH ₂ -bridge	10.6/12.0	18.0/19.6	-7.9/-6.4
M ^{IV} -C ₆ H ₁₂ → M ^{IV} -C ₈ H ₁₆	CMe ₂ -bridge	9.5/7.3	15.8/15.4	-7.4/-7.6
7C + C ₂ H ₄ → 7C-E → 9C	CMe ₂ CH ₂ -bridge	9.0/8.8	17.4/18.6	-7.4/-6.2
M ^{IV} -C ₈ H ₁₆ → M ^{IV} -C ₁₀ H ₂₀	CMe ₂ -bridge	15.7/14.7	20.1/18.4	-9.3/-10.4
9C + C ₂ H ₄ → 9C-E → 11C	CMe ₂ CH ₂ -bridge	14.3/13.4	20.7/19.8	-10.3/-11.4

^a The activation and reaction free energies for individual processes are given for Zr/Hf-based catalysts, respectively, relative to {corresponding metallacycle precursor **XC** + C₂H₄}. ^b Stabilization of the ethylene π -adduct **XC-E** (with X = 5, 7, 9, respectively).

odology (DFT(BP86) + valence triple- ζ basis sets) to allow us to draw mechanistic conclusions having substantial predictive value.

Basis sets of valence triple- ζ quality for all elements^{32b} together with a quasi-relativistic ECP for group 4 elements³³ were employed in the geometry optimization and transition state localization. The frequency calculations were conducted by using the same basis set for group 4 elements,³³ but split-valence basis sets^{32a} for the main group elements for structures localized at this level. Further details of the computational procedure were reported elsewhere.^{14b}

Stationary Points. The geometry optimization and the saddle-point search were carried out by utilizing analytical/numerical gradients/Hessians according to standard algorithms. No symmetry constraints were imposed in any case. The stationary points were identified exactly by the curvature of the potential-energy surface at these points corresponding to the eigenvalues of the Hessian. All reported transition states possess exactly one negative Hessian eigenvalue, while all other stationary points exhibit exclusively positive eigenvalues. The reaction and activation free energies (ΔG , ΔG^\ddagger at 298 K and 1 atm) were evaluated according to standard textbook procedures³⁴ using computed harmonic frequencies. The effect of the solvent and the counterion was neglected in the present study; the rationale behind them can be found elsewhere.^{14a,b} For the oligomerization to occur in liquid phase,^{12d} the solvation entropy for olefin association and dissociation was approximated as being 2/3 of its gas-phase value. The authors consider this a reliable estimate of the entropy contribution in the condensed phase; further details were reported elsewhere.^{14b}

To keep the notation consistent with previous studies,¹⁴ the key species of the oligomerization process were labeled with the following notation (cf. Scheme 1): viz., the (ethylene)₂-M^{II} active catalyst complex **2**, the metalla(IV)cycloalkanes **XC**; the respective ethylene π -adducts **XC-E**; the α -olefin-M^{II} complex **XC-O**. The notation **X** = **5**, **7**, **9** was used to indicate whether five-, seven-, or nine-membered metallacycle intermediates, i.e., metalla(IV)cyclopentane, -heptane, or -nonane, respectively, were involved. The key species encountered along the stepwise degradation of the metalla(IV)cyclopentane **5C** were labeled as follows: the transition state for β -H abstraction **T5C-HA** and reductive CH elimination **T5C-HRE**, and the alkenyl-hydride-M^{IV} intermediate **5C-H**. The localized key species for the corresponding Zr and Hf systems exhibit a very

similar structural characteristic. We, therefore, decided to restrict the presentation of key structures for the individual elementary steps to those for the Zr catalyst as a representative example.

Results and Discussion

We shall focus here on the **2** → **5C** oxidative coupling to afford the first metalla(IV)cyclopentane and the subsequent growth and decomposition steps for various metallacycle intermediates up to the nine-membered ring. The kinetically determined propensity of the metalla(IV)cycloheptane, **7C**, and -nonane, **9C**, intermediates to either grow or decompose has been analyzed to control the distribution of oligomer products in the valuable range of C₆-C₁₈ chain lengths.^{14b} The sequence of steps passing through along the favorable route for precatalyst activation has been examined previously in great detail.^{14b} First, crucial structural and energetic aspects of critical elementary steps will be discussed for the boratabenzene systems and compared to parent Cp analogues. This might bring us in a position to suggest promising catalyst modifications aimed at improving their catalytic abilities. The free-energy profile for the first formation of **5C** and its subsequent enlargement into **7C** and **9C** is collected in Table 1, while the energetics for the metallacycle decomposition is summarized in Table 2.

As a general feature, the boratabenzene ligand preferably adopts an almost planar conformation, maintaining an η^6 hapticity of the boratabenzene-M coordination in the most stable isomer for each of the investigated key species. No remarkable distortion or ring slippage of the boron cycle has been found in any of the located key species.³⁵

I. Examination of Critical Elementary Steps. A. Formation of the First Metalla(IV)cyclopentane.

Commencing from the active catalyst complex **2**, formation of the first metalla(IV)cyclopentane **5C** takes place through oxidative coupling of the two ethylene moieties (cf. Scheme 1). The corresponding transition state TS-[**2**-**5C**] emerges at a distance of ~ 2.0 Å for the newly formed C-C bond between two coplanar ethylenes,

(32) (a) Schäfer, A.; Huber, C.; Ahlrichs, R. *J. Chem. Phys.* **1992**, *97*, 2571. (b) Schäfer, A.; Huber, C.; Ahlrichs, R. *J. Chem. Phys.* **1994**, *100*, 5829. (c) Eichkorn, K.; Treutler, O.; Öhm, H.; Häser, M.; Ahlrichs, R. *Chem. Phys. Lett.* **1995**, *240*, 283. (d) Eichkorn, K.; Weigend, F.; Treutler, O.; Ahlrichs, R. *Theor. Chim. Acta* **1997**, *97*, 119. (e) TURBOMOLE basis set library.

(33) (a) Dolg, M.; Wedig, U.; Stoll, H.; Preuss, H. *J. Chem. Phys.* **1987**, *86*, 866. (b) Andrae, D.; Häussermann, M.; Dolg, M.; Stoll, H.; Preuss, H. *Theor. Chim. Acta* **1990**, *77*, 123.

(34) McQuarrie, D. A. *Statistical Thermodynamics*; Harper & Row: New York, 1973.

(35) (a) Although ring slippage is a well-known, facile process in various Cp-based and analogues complexes, isomers that are characterized by a diminished hapticity of the boratabenzene-M interaction (M = Zr, Hf) were generally found to be energetically less favorable. Therefore, only species with a η^6 -boratabenzene-M fragment will be discussed in the present work. (b) For facile ring slippage processes, see for instance: O'Connor, J. M.; Casey, C. P. *Chem. Rev.* **1987**, *87*, 307.

Table 2. Calculated Gibbs Free-Energy Profile (ΔG , ΔG^\ddagger in kcal mol⁻¹) for Decomposition of Group 4 Metallacycle Intermediates Affording α -Olefins during the Linear Oligomerization of Ethylene Mediated by the Cationic $[(\eta^6\text{-BC}_5\text{H}_5\text{-}(\text{R-bridge})\text{-C}_6\text{H}_5)\text{M}^{\text{II}}(\text{C}_2\text{H}_4)_2]^+$ ($\text{M} = \text{Zr, Hf}$) Active Catalyst Complex^a

cycle decomposition	R-bridge	ΔG^\ddagger , M = Zr/Hf	ΔG , M = Zr/Hf	$\Delta\Delta G_{\text{d-g}}^{\ddagger, 40}$ M = Zr/Hf
$\text{M}^{\text{IV}}\text{-C}_4\text{H}_8 \rightarrow 1\text{-butene-M}^{\text{II}}$	$\text{CMe}_2\text{-bridge}$	26.2/27.5 ^b	2.8/11.8	11.7/11.7
5C \rightarrow 5C-O	$\text{CMe}_2\text{CH}_2\text{-bridge}$	28.6/29.7 ^b	2.5/10.4	10.6/10.1
$\text{M}^{\text{IV}}\text{-C}_6\text{H}_{12} \rightarrow 1\text{-hexene-M}^{\text{II}}$	$\text{CMe}_2\text{-bridge}$	10.0/13.4	-13.9/-9.6	-5.8/-2.0
7C \rightarrow 7C-O	$\text{CMe}_2\text{CH}_2\text{-bridge}$	7.4/11.5	-15.9/-11.7	-10.0/-7.1
$\text{M}^{\text{IV}}\text{-C}_8\text{H}_{16} \rightarrow 1\text{-octene-M}^{\text{II}}$	$\text{CMe}_2\text{-bridge}$	14.2/16.6	-17.7/-13.4	-5.9/-1.8
9C \rightarrow 9C-O	$\text{CMe}_2\text{CH}_2\text{-bridge}$	13.5/16.1	-19.9/-16.7	-7.2/-3.7

^a The activation and reaction free energies for individual processes are given for Zr/Hf-based catalysts, respectively, relative to the corresponding metallacycle precursor **5C**. ^b Only the barrier for the kinetically more difficult first β -H abstraction of the stepwise mechanism is given.

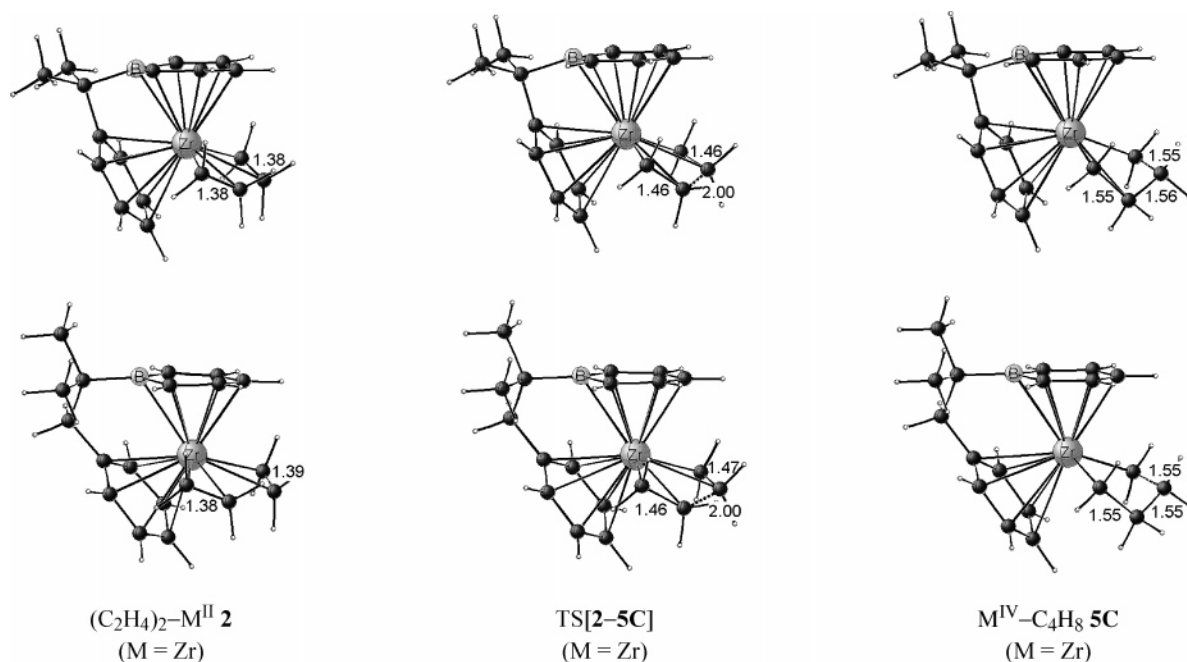


Figure 2. Selected geometric parameters (Å) of the optimized structures of key species for oxidative coupling of two ethylene moieties in **2** to afford the metalla(IV)cyclopentane **5C**, for CMe_2 -bridged (top) and CMe_2CH_2 -bridged (bottom) systems, exemplified for Zr catalysts. The cutoff for drawing M-C bonds was arbitrarily set at 2.8 Å.

which decays into **5C**. As evident from the key species shown in Figure 2, the ancillary phenyl group does not undergo any significant change of its coordination mode along the **2** \rightarrow **5C** transformation, for both the C₁- and C₂-bridged systems. This is different from what we found for the parent Cp-based systems,^{14b} where the decay of the transition state into the metalla(IV)-cyclopentane goes along with reduction of the hapticity of the phenyl-M coordination, thus adopting an η^1 -mode in **5C**. The stronger η^6 phenyl-M coordination in **5C** when compared to the parent $\text{CpM}^{\text{IV}}\text{-C}_4\text{H}_8$ species can be attributed to the higher electrophilicity of the metal in **5C** (cf. the introductory part), which causes an amplified arene-M interaction.

The oxidative coupling is found to be kinetically the most easy step overall of all crucial elementary processes. This process requires to overcome a free-energy barrier of 9.2–10.7 kcal mol⁻¹ and is driven by a thermodynamic force of -(5.5–8.0) kcal mol⁻¹ (cf. Table 1). This indicates the **2** \rightarrow **5C** step as a highly facile, essentially irreversible process. Accordingly, **2** can be assumed, after its generation during the initial precatalyst activation period, to become readily and almost quantitatively transformed into **5C**.

The very narrow range predicted for the activation and reaction free energies for all investigated catalysts shows that both the metal as well as the length of the bridge influence the energetics of the oxidative coupling to only a minor extent. Interestingly, as revealed from the comparison with the parent Cp analogues,^{36a} the electronic modification of the Cp ligand by boron substitution does not affect the energy profile significantly either, which is in contrast to the findings for the subsequent metallacycle growth and decomposition steps (vide infra).

(36) This is exemplified for the $[(\eta^5\text{-C}_5\text{H}_4\text{-}(\text{CMe}_2\text{-bridge})\text{-C}_6\text{H}_5)\text{M}^{\text{II}}(\text{C}_2\text{H}_4)_2]^+$ ($\text{M} = \text{Zr, Hf}$) active catalysts explored in previous studies (refs 14b,c). (a) The free-energy barrier for **2** \rightarrow **5C** oxidative coupling amounts to 11.1/9.4 kcal mol⁻¹, while that for ethylene insertion into the M^{IV}-C bond of various metalla(IV)cycloalkanes is 11.5/11.8 (into **5C**), 14.5/15.7 (into **7C**), and 17.3/17.4 (into **9C**) kcal mol⁻¹ for Zr/Hf systems, respectively. (b) For the stepwise decomposition of **5C** free-energy barriers of 21.1/23.5 kcal mol⁻¹ (β -H abstraction) and 21.4/25.7 kcal mol⁻¹ (reductive CH elimination) have to be overcome for Zr/Hf systems, respectively, with the intervening alkenyl-hydride-M^{IV} intermediate at 19.9/22.4 kcal mol⁻¹. All energetics are relative to **5C**. (c) The decomposition via the concerted β -H transfer is connected with free-energy barriers of 13.1/17.4 (**7C**) and 16.1/20.1 (**9C**) kcal mol⁻¹ for Zr/Hf systems, respectively. This occurs in an exergonic process that is driven by a thermodynamic force of -9.0/-3.7 (**7C**) and -15.3/-10.1 (**9C**) kcal mol⁻¹, respectively.

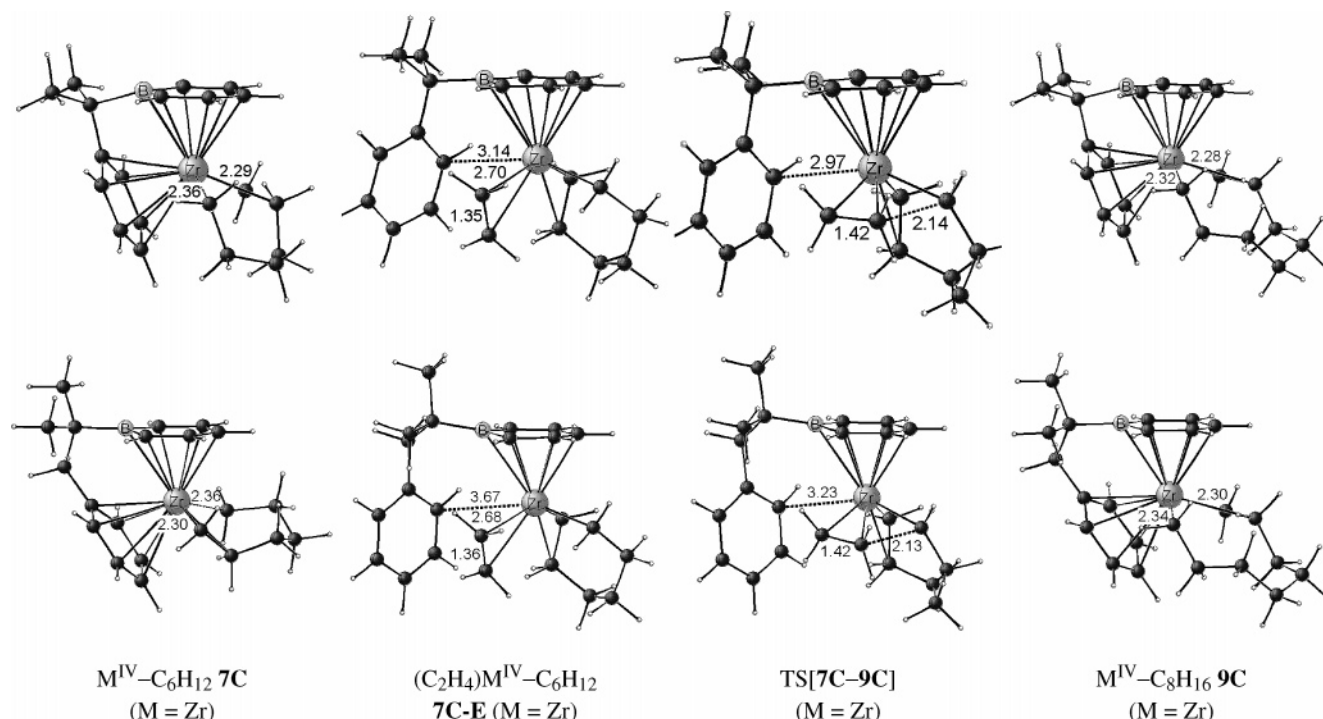


Figure 3. Selected geometric parameters (Å) of the optimized structures of key species for ethylene insertion into the $M^{IV}-C$ bond of the metalla(IV)cycloheptane **7C** giving rise to the metalla(IV)cyclononane intermediate **9C**, for CMe_2 -bridged (top) and CMe_2CH_2 -bridged (bottom) systems, exemplified for Zr catalysts. The cutoff for drawing $M-C$ bonds was arbitrarily set at 2.8 Å.

B. Growth of Metallacycle Intermediates. The increase of the metallacycle's ring size occurs via the repeated ethylene uptake and subsequent insertion into the $M^{IV}-C$ bond of the metalla(IV)cycloalkane intermediate. The overall highest barrier of this process is connected with the insertion, while the uptake requires surmounting a significantly lower barrier.^{14a} The key species for the $7C + C_2H_4 \rightarrow 9C$ process are displayed in Figure 3, exemplified for CMe_2 - and CMe_2CH_2 -bridged Zr catalysts. The transition state encountered along the most feasible pathway comprises a quasi-planar four-membered *cis* arrangement of the metallacycle's $M^{IV}-C$ bond, the coplanar-oriented ethylene monomer, and the metal, which leads to a new C_2 -extended metallacycle in the final stage of the process.

As revealed from Figure 3, the process to enlarge the metallacycle size is accompanied by the displacement of the ancillary arene functionality by the incoming ethylene. Commencing from the metalla(IV)cycloalkane precursor **XC**, where for both C_1 - and C_2 -bridged systems the phenyl- M^{IV} coordination is slightly unsymmetrical, but still centrosymmetric, the first ethylene uptake gives rise to a weakly bound ethylene π -encounter complex **XC-E**. The ancillary arene functionality maintains only a loose contact to the metal in the species **XC-E**. The phenyl group still resides outside of the direct metal's coordination sphere during the insertion process until it approaches the transition state, before becoming reattached after completion of the process with the decay of the TS into the next larger metalla(IV)cycloalkane.

The first phenyl group displacement by incoming ethylene during the encounter complex generation has been analyzed in previous studies¹⁴ to contribute mostly to the relative overall barrier, while the intrinsic

insertion barrier, i.e., for the formal **XC-E** \rightarrow **TS[XC-(X+2)C]** process, is a smaller part that was found to be influenced to only a minor extent by electronic modifications of the arene functionality.^{14c} Accordingly, the kinetics of the metallacycle growth is decisively determined by the strength of the arene- M^{IV} interaction in **XC**. As a further aspect, the ligand reorganization associated with the growth step is found to be affected by the metallacycle size. Modest reorganizations can be observed for ethylene complexation to the two smallest **5C** and **7C**, while for **9C** a larger rearrangement of the ligand sphere is required. As a result, ethylene coordinates most strongly to **5C** and **7C** (although this is still unfavorable at the free-energy surface, Table 1), which moreover leads to a kinetically more easy insertion, when compared to the process commencing from **9C**. These observations parallel the findings for the parent Zr and Hf Cp-based systems, but contrast that for the Cp-Ti catalyst.^{14b} Thus, this behavior can be traced back to the larger ionic radius of the heavier group 4 metals, as already analyzed in great detail previously.^{14b}

The kinetics of the insertion process displays the following trends (cf. Table 1). (1) Very similar energetics is predicted for the corresponding Zr and Hf catalysts, thereby indicating that this step is influenced to only a minor extent by whether Zr or Hf is the active center. (2) The increase of the five- and seven-membered cycles is most facile, needing to overcome a similar activation barrier that amounts to 14.5–15.8 kcal mol⁻¹ (ΔG^\ddagger) for C_1 -bridged and 17.4–19.6 kcal mol⁻¹ (ΔG^\ddagger) for C_2 -bridged systems. The growth of the next larger intermediate, **9C**, is predicted to be distinctly more difficult ($\Delta G^\ddagger = 18.4$ –20.1 kcal mol⁻¹) for catalysts with a C_1 -bridge, which is due to the larger reorganization of the ligand sphere required in this case (vide supra). This

kinetic gap, however, diminishes for C₂-bridged compounds, as here sterics come into play (vide infra). (3) The larger insertion barrier for catalysts bearing an extended C₂-bridge, when compared to the corresponding C₁ systems, can be attributed to two factors. First, this bridge amplifies the M^{IV}-arene coordination in the precursor **XC**, as it acts to increase the flexibility of the phenyl group to adopt the most favorable position. This renders the necessary arene displacement more expensive energetically. Second, the incoming ethylene interacts more strongly with the C₂-bridged phenyl group, which is indicated by the larger distance of the nearest phenyl-M contact found for both the encounter complex and the transition state (cf. Figure 3). Both factors contribute to the increase of the barrier for ethylene insertion into **5C** and **7C** by ~3 kcal mol⁻¹ ($\Delta\Delta G^\ddagger$), when compared to the C₁-bridged counterparts. In contrast, unfavorable steric interactions between the extended C₂-bridge and the nine-membered metallacycle act to destabilize **9C**, thus giving rise to a comparable activation energy for both C₁- and C₂-bridged systems in this case. (4) The comparison with the Cp-based analogues revealed that for boratabenzene catalysts the growth step is, in general, more complicated kinetically,^{36a} provided that unfavorable steric interactions between the metallacycle fragment and the ligand sphere are not effective. Here, the higher electrophilicity of the metal center caused by the boron-substituted Cp moiety is the major factor that rationalizes these findings.

Variation of the active metal center is seen to have a rather small influence on the thermodynamics of the growth process, as the thermodynamic driving force is predicted to be similar for the Zr and Hf systems of the respective catalysts (cf. Table 1). Overall, growth of the five-, seven-, and nine-membered zircona(IV)- and hafnia(IV)cycles is an exergonic and essentially irreversible process, such that thermodynamics are not likely to prevent metallacycle growth, and thereby not acting to regulate the α -olefin product distribution.

C. Decomposition of Metallacycle Intermediates to Afford α -Olefins. Depending on the size of the metallacycle, the decomposition of group 4 metalla(IV)-cycloalkanes follows two distinct mechanisms, which parallels the findings for the parent Cp-based systems.¹⁴ The stepwise mechanism comprised of β -H abstraction and subsequent reductive CH elimination with an intervening alkenyl-hydride-M^{IV} species involved is favorable for the smallest, thus rigid, intermediate **5C**. By contrast, for the conformationally flexible cycles starting with **7C** the concerted β -H transfer, taking place in close proximity to the metal, is operative.

Starting with the decomposition of **5C**, this multistep process exhibits a double-valley energy profile. The first β -H abstraction is seen to come at the expense to the arene-M interaction.³⁷ The ancillary phenyl group preferably adopts the η^1 -mode in **T5C-HA** for both CMe₂- and CMe₂CH₂-bridged catalysts. Following the reaction path the η^2, η^1 -alkenyl-hydride-M^{IV} intermediate **5C-H** is encountered next, which is stabilized by the reattached η^6 -arene functionality. The decomposition is completed after passing through **T5C-HRE**, which is

reached at a distance of ~1.9 Å of the emerging CH bond, giving rise to the $[(\eta^6\text{-BC}_5\text{H}_5\text{-}(\text{bridge})\text{-}\eta^6\text{-C}_6\text{H}_5)\text{-M}^{\text{II}}]^+$ complex under liberation of 1-butene. The structures of the key species involved in the **5C** decomposition are shown in Figure S1 of the Supporting Information.

The computed energetics resembles the structural aspects discussed thus far (cf. Table 2). The first step is connected with a prohibitively large barrier of 26.2/27.5 and 28.6/29.7 kcal mol⁻¹ ($\Delta\Delta G^\ddagger$) for Zr/Hf systems with a C₁- and C₂-bridge, respectively. This points out that the β -H abstraction is distinctly more difficult kinetically for boratabenzene catalysts than for the Cp-based analogues,^{36b} owing to the reduction of the hapticity of the arene-M coordination associated with the former systems. The **5C-H** intermediate is found to be 17.5–20.9 (C₁-bridge) and 15.4–19.3 (C₂-bridge) kcal mol⁻¹ higher in free energy relative to **5C**. This species is indicated to be highly reactive, thus being not likely to occur in appreciable concentrations, as **5C-H** is separated from **T5C-HRE** by only 2–3 kcal mol⁻¹. The reductive CH elimination is predicted to be the kinetically less expensive of the two consecutive steps, having a free-energy barrier of 18.7/22.8 (C₁-bridge) and 16.6/21.3 (C₂-bridge) kcal mol⁻¹ for Zr/Hf catalysts, respectively. This contrasts with the situation for the related Cp-based systems, where the two subsequent steps have similar kinetics.¹⁴ The increase of the elimination barrier in the Hf > Zr order can be rationalized by the enhanced M-C bond strength upon descending group 4.³⁸ As clearly revealed from the geometry of **T5C-HRE** (cf. Figure S1), here, the hemilabile arene functionality, in contrast to the insertion step (cf. section I.B), acts to support the transition state coordinatively. The larger flexibility of the C₂-bridged phenyl group allows a more efficient stabilization of **T5C-HRE**, without introducing unfavorable steric interactions with the smallest five-membered metallacycle, thus serving to accelerate the process when compared to C₁-bridged systems. As a further aspect, the elimination rate can be controlled also by the ability of a suitably modified Cp moiety to support the formal M^{IV} → M^{II} process electronically. The low lying boratabenzene σ -acceptor orbital^{23,24} plays a pivotal role in this regard, giving rise to a free-energy barrier that is 2.5–3.0 kcal mol⁻¹ lower relative to the analogous Cp catalysts.^{36b}

The key species for the **7C** decomposition into the 1-hexene-M^{II} product **7C-O** through concerted transition-metal-assisted β -H transfer are shown in Figure 4, exemplified for the CMe₂- and CMe₂CH₂-bridged Zr catalysts. The transition state for the transfer of a hydrogen atom between the C ^{β} and C ^{α'} carbons constitutes a quasi-planar arrangement of the MC ^{β} HC ^{α'} fragment and occurs halfway between educt and product, i.e., with similar C ^{β} -H and C ^{α'} -H distances. Similar to the CH elimination along the stepwise pathway, the phenyl ligand assists the β -H transfer, first, by stabilizing the transition state coordinatively by the compensation for the reduction of the coordination sphere around the metal, and second, by the

(37) Of several attempts undertaken, we have not been able to localize an isomer of **T5C-HA** with a strongly centrosymmetrically coordinated phenyl group.

(38) (a) Mingos, D. M. P. *Essential Trends in Inorganic Chemistry*; Oxford University Press: Oxford, U.K., 1998. (b) Elschenbroich, Ch.; Salzer, A. *Organometallics: A Concise Introduction*, 2nd ed.; Wiley-VCH: Germany, 1992.

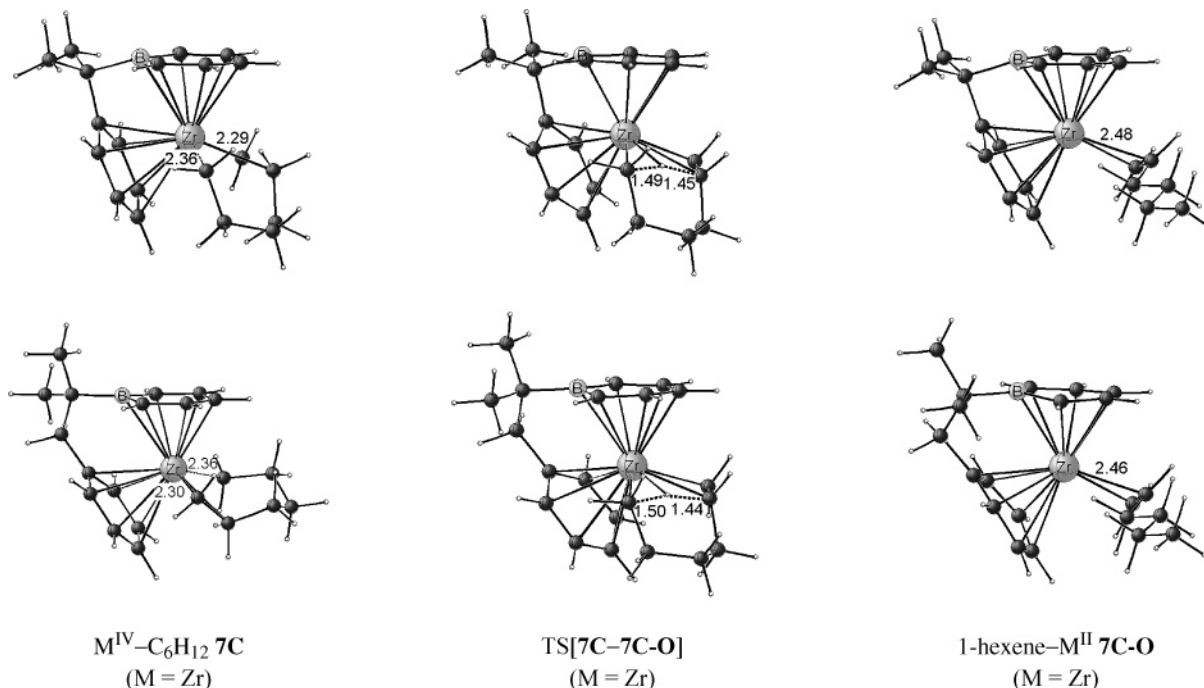


Figure 4. Selected geometric parameters (Å) of the optimized structures of key species for decomposition of the metalla-(IV)cycloheptane **7C** into the 1-hexene-M^{II} complex **7C-O** through concerted transition-metal-assisted β -H transfer, for CMe₂-bridged (top) and CMe₂CH₂-bridged (bottom) systems, exemplified for Zr catalysts. The cutoff for drawing M-C bonds was arbitrarily set at 2.8 Å.

support of the metal's low oxidation state in the α -olefin-M^{II} products **XC-O**.

Overall, and in analogy with the observation for the Cp-based congeners,¹⁴ decomposition of larger cycles starting with **7C** becomes significantly accelerated along the concerted pathway (cf. Table 2). The largest barriers of 13.4 and 16.6 kcal mol⁻¹ (ΔG^\ddagger , Table 2) for the 1-hexene and 1-octene production paths, respectively, clearly indicate that the two processes are being facile. Following the argument concerning the stability of the M-C bond and the flexibility of the bridge given before, the trend in the predicted kinetics for individual catalysts becomes understandable (cf. Table 2). (1) Decomposition of **7C** is the most easy kinetically among all investigated metallacycles, while the 1-octene generation is connected with a ~ 3 –6 kcal mol⁻¹ higher barrier. This is so, because TS[**7C**-**7C-O**] adopts a highly stable conformation,³⁹ while for larger rings close H-H contacts within the metallacycle fragment lead to a destabilization of the respective transition states. (2) The increase of the M-C bond strength upon descending group 4 causes the barrier for Hf catalysts to be higher than for Zr counterparts. (3) Catalysts bearing a flexible CMe₂CH₂-bridge display a higher propensity for decomposition of **7C** than their C₁-bridged congeners. This preference, however, is no longer seen for **9C**, where very similar barriers are predicted for the corresponding C₁- and C₂-bridged catalysts, since here unfavorable steric interactions between the arene and metallacycle moieties appear as a counterbalancing factor. (4) Most remarkably, however, the boron substitution of the Cp moiety leads, in general, to a distinct acceleration of the metallacycle degradation. There are two factors that

govern the decrease of the activation free energy by ~ 2 –4 kcal mol⁻¹ ($\Delta\Delta G^\ddagger$, Table 2)^{36c} relative to the Cp-based catalysts. The aforementioned low-lying σ -acceptor orbital and also the higher electrophilicity of the metal support the reductive β -H transfer, thereby making the metallacycle decomposition, in contrast to the growth (cf. section I.B), kinetically easier. As a further aspect, generation of the α -olefin-M^{II} products **XC-O** is seen to be a strongly exergonic process, driven by a large thermodynamic force (cf. Table 2). In addition to the kinetic preference, the decomposition is facilitated also thermodynamically for boratabenzene catalysts,^{36c} owing to an enhanced σ -donating interaction in the **XC-O** products.

II. Influence of the Electronic Modification of the Cyclopentadienyl Moiety on the Catalyst's Ability for Linear Oligomerization of Ethylene. Having gauged the influence of the electronic modification of the Cp moiety on the energy profile for crucial steps, we are now at the position to estimate the catalytic potential of the, yet hypothetical, group 4 mono(boratabenzene-arene) catalysts for linear oligomerization of ethylene. The distribution of the oligomer products has been shown previously^{14b} to be almost entirely regulated kinetically by the propensity of the individual metallacycle intermediates to either decompose or grow, which is indicated by the $\Delta\Delta G^\ddagger_{d-g}$ value⁴⁰ reported in Table 2.

Starting with the Zr-mediated oligomerization, degradation of **5C**, which is readily formed via **2** \rightarrow **5C** oxidative coupling (cf. section I.A), along a stepwise pathway is entirely suppressed by an insurmountable high barrier for the first β -H abstraction (cf. section I.C),

(39) The favorable conformation of TS[**7C**-**7C-O**] resembles formally similarity to the chair conformation of cyclohexane (cf. Figure 4), which makes its particular stability understandable.

(40) The $\Delta\Delta G^\ddagger_{d-g}$ value represents the difference of the free-energy barriers for competing decomposition and growth steps for a particular metallacycle intermediate.

thereby forcing **5C** to grow and precluding the generation of 1-butene as an oligomerization product. The next larger zircona(IV)cycle **7C** and also **9C** display a distinctly higher propensity to decompose than to undergo further ethylene insertion events. The $\Delta\Delta G_{d-g}^{\ddagger}$ value for **7C** of -5.8 kcal mol $^{-1}$ predicted for the C₁-bridged Zr catalyst, which becomes even larger for the counterpart bearing the extended C₂-bridge (-10.0 kcal mol $^{-1}$, Table 2), can be considered as being large enough to prevent any further increase of the metallacycle completely.⁴¹ As a consequence, (1) **7C** is the largest zircona(IV)cycle intermediate occurring in appreciable concentrations during the reaction course, and (2) 1-hexene is almost exclusively formed among the various possible oligomers. Furthermore, the **5C** + C₂H₄ → **7C** cycle growth is the rate-controlling step that is connected with a free-energy barrier of 14.5 (C₁-bridge) and 18.0 (C₂-bridge) kcal mol $^{-1}$ (cf. Table 1), respectively. For the experimentally reported [(η^5 -Cp-(CMe₂-bridge)-C₆H₅)-Ti^{II}-(C₂H₄)₂]⁺ active trimerization catalyst^{12a,b} this barrier amounts to 15.5 kcal mol $^{-1}$.^{14b} This leads us to conclude that (1) the two probed Zr systems should display catalytic abilities for the selective ethylene trimerization to 1-hexene and that (2) the C₁-bridged mono(boratabenzene-arene) Zr catalyst is likely to be highly efficient, exhibiting an activity that is beyond what is reported for the established Cp-based Ti catalyst.^{12a,b}

In analogy with the situation for Zr systems analyzed thus far, the path for 1-butene production is entirely suppressed for the Hf-supported reaction as well, owing to the clear preference of **5C** to grow further ($\Delta\Delta G_{d-g}^{\ddagger} = 10.1$ – 11.7 kcal mol $^{-1}$). Concerning the oligomerization abilities, the C₂-bridged Hf system bears great similarity to the Zr catalysts. The $\Delta\Delta G_{d-g}^{\ddagger}$ gap for **7C**, predicted as being as large as -7.1 kcal mol $^{-1}$ (cf. Table 2),⁴¹ clearly points out that this compound is likely to be a trimerization catalyst. However, this catalyst might be a less favorable alternative to the aforementioned C₁-bridged Zr analogue, as the ethylene insertion has been shown in section I.B to be kinetically more expensive upon descending group 4 and also for systems with an extended C₂-bridge. Indeed, the barrier for the rate-determining **5C** + C₂H₄ → **7C** step amounts to 19.6 kcal mol $^{-1}$ (cf. Table 1), thereby suggesting that this Hf system (C₂-bridge) is a significantly less active trimerization catalyst.

A different product composition is suggested for the C₁-bridged Hf catalyst. In this case, comparable barriers are predicted for ethylene insertion and concerted β -H transfer for **7C** and **9C**, with the two hafnia(IV)cycles exhibiting a moderately higher propensity for decomposition ($\Delta\Delta G_{d-g}^{\ddagger} = -2.0$ and -1.8 kcal mol $^{-1}$, respectively; cf. Table 2). Although **7C** is slightly more likely to decompose, there is also a probability for formation of **9C**, such that 1-hexene would be the major product, together with some amount of 1-octene. This parallels our findings for the Cp-based Zr analogue (C₁-bridge), which has been suggested as a promising catalyst possessing abilities for generation of 1-octene besides the prevalent 1-hexene oligomer product.^{14b} As already

mentioned in the Introduction, the substituent on boron might be an efficient handle for tuning the $\Delta\Delta G_{d-g}^{\ddagger}$ gap for boratabenzene catalysts. According to our experience with the Cp analogue systems, this is likely to influence the gap congruously for both **7C** and **9C**. Thus, a suitably modified boratabenzene ligand can act to modulate the oligomer product composition toward an enhanced 1-octene portion, which leads in the best of cases to comparable amounts of 1-hexene and 1-octene. Although the relative α -olefin proportions can be tuned to some degree, this, unfortunately, does not offer a strategy for the making 1-octene the entire or even the predominant product of the ethylene oligomerization process.

Concluding Remarks

We have presented a detailed computational exploration of the catalytic abilities of group 4 mono(boratabenzene-arene) Zr and Hf compounds for linear ethylene oligomerization, employing a gradient-corrected DFT method. This study was aimed at probing computationally the potential of an electronically modified, viz., boron-substituted, Cp moiety in the parent group 4 [(η^5 -Cp-(bridge)-Ph)M^{II}-(C₂H₄)₂]⁺ active catalyst species, where the C₁-bridged Ti compound was recently described as an effective trimerization catalyst,^{12a,b} to act to increase the catalytic activity and/or to modulate the α -olefin distribution. This allowed us to contribute to the computer-based rational design of improved group 4 oligomerization catalysts by suggesting Zr and Hf boratabenzene compounds with a hemilabile arene functionality that (1) are a more efficient alternative to the reported Cp-based Ti trimerization catalyst^{12a,b} or (2) have the promising ability for generation of both 1-hexene and 1-octene.

The influence of the boron substitution of the cyclopentadienyl moiety on the energy profile of important elementary steps can be summarized as follows: (1) The highly facile **2** → **5C** oxidative coupling is the step that is least affected overall by this modification. Almost identical energetics is predicted for the boratabenzene and the corresponding Cp-based systems. (2) The ethylene uptake and insertion into the M^{IV}-C bond is accompanied by the displacement of the hemilabile phenyl ligand by the incoming ethylene. Therefore, the strength of the M^{IV}-arene interaction in the metallacycle precursors **XC** is the crucial factor that mainly determines the kinetics of the metallacycle growth. The higher electrophilicity of the metal center in the boratabenzene compounds causes a strong η^6 M^{IV}-phenyl coordination in **XC**, which makes the increase of the metallacycle more complicated kinetically, provided that unfavorable sterics are not effective. (3) The concerted β -H transfer is supported by both the reduced donor ability and the low lying σ -acceptor orbital of the boratabenzene ligand. This leads, in contrast to the growth step, to a pronounced acceleration of the metallacycle decomposition.

With regard to the catalytic potential of the probed Zr and Hf boratabenzene systems, the C₁-bridged Zr compound is likely to be a highly efficient catalyst for ethylene trimerization, which should exhibit an activity that exceeds what is reported for the established Cp-based Ti catalyst.^{12a,b} A different product distribution

(41) For the purpose of comparison only, the $\Delta\Delta G_{d-g}^{\ddagger}$ gap has been predicted to amount to -6.1 kcal mol $^{-1}$ (ref 14b) for the experimentally established [(η^5 -Cp-(CMe₂-bridge)-C₆H₅)-Ti^{II}-(C₂H₄)₂]⁺ active trimerization catalyst reported by Hessen and co-workers (refs 12a,b).

is predicted for the Hf counterpart. This system is suggested as possessing catalytic potential for production of 1-octene besides the prevalent 1-hexene oligomer product. Electronic modification of the substituent on boron can act to modulate the α -olefin product composition toward an enhanced 1-octene portion, although not as the predominant product.

Acknowledgment. Support from the National Science and Engineering Research Council of Canada (NSERC) is gratefully acknowledged. T.Z. wishes to

thank the Canadian government for a Canada research chair in theoretical inorganic chemistry.

Supporting Information Available: Full descriptions of the geometry of all reported species (Cartesian coordinates in Å). Also included is the pictorial representation of key species for decomposition of the metalla(IV)cyclopentane intermediate **5C** (Figure S1). This material is available free of charge via the Internet at <http://pubs.acs.org>.

OM049362W